# Analysis of the influence of joint direction on production optimization in enhanced geothermal systems

Dorcas S. Eyinla[1,2,3] ®

## Abstract

Heat extraction from geothermal reservoir by circulating cold water into a hot rock requires an amount of fluid pressure, which is capable of inducing fault opening. Although stress change promotes the potential of fault failure and reactivation, the rate at which fluid pressurization within the fault zone generates variations in pore pressure as fault geometry changes during geothermal energy production have not been thoroughly addressed to include the effects of joint orientation. This study examines how different fault/joint models result in different tendency of injection-induced shear failure, and how this could influence the production rate. Here, a numerical simulation method is adopted to investigate the thermo-hydro-mechanical (THM) response of the various fault/joint models during production in a geothermal reservoir. The results indicate that pore pressure evolution has a direct relationship with the evolution of production rate for the three joint models examined, and the stress sensitivity of the individual fault/joint model also produced an effect on the production rate. Changing the position of the injection well revealed that the magnitude of shear failure on the fault plane could be controlled by the hydraulic diffusivity of fluid pressure, and the production rate is also influenced by the magnitude of stress change at the injection and production wells. Overall, the location of the injection well along with the fault damage zone significantly influenced the resulting production rate, but a more dominating factor is the joint orientation with respect to the maximum principal stress direction. Thus, the rate of thermal drawdown is affected by pore pressure elevation and stress change while the fault permeability and the production rate are enhanced when the joint's frictional resistance is low.

**Keywords** Production rate evolution · Joint orientation · Stress state · Pressure drawdown · Frictional resistance

## Introduction

A major setback in developing enhanced geothermal systems, shale gas, and tight hydrocarbon reservoir is the understanding of fracture network and possibilities of enhancing permeability of the fractured reservoir (Eshiet and Sheng 2017). Hence, knowledge of the variations in these properties is fundamental in characterising fractured reservoirs because they possess a direct correlation with the magnitude of fracture opening and production rate (Men et al. 2018). The poroelastic effect caused by pressure build-up varies as the injection condition changes; consequently, when injecting into a low-permeable fault and fluid pressure is induced, the hydraulic diffusivity of the fluid pressure would be dependent on several factors such as the position of the injector, and the velocity of fluid transmission (Vilarrasa et al. 2016; Eyinla et al. 2020, 2021a; Eyinla 2021; Eyinla and Oladunjoye 2021). However, the joint direction has been described as one of the factors which influences the instability of a fault and determines the fault reactivation potential and the rate of stress change during fault loading (Streit and Hillis 2004; Eyinla and Oladunjoye 2021).

Computational approach provides an insight into the mechanics of deformational sequence in fault under stress, and thus impacts on the permeability (Lavrov 2017). Operationally, fluid injection is a process adopted for optimizing recovery in tight reservoir, especially in enhanced

✉ Dorcas S. Eyinla
dorcas.eyinla@aaua.edu.ng

1 Department of Geology, Pan African University, Life and Earth Sciences Institute (PAULESI), University of Ibadan, Ibadan, Nigeria

2 Department of Earth Sciences, Adekunle Ajasin University, Akungba Akoko, Nigeria

3 Department of Petroleum Geology and Geology, School of Geosciences, University of Aberdeen, Aberdeen, Scotland, UK

geothermal systems, and it has improved drastically in the past decades. It has also positively impacted the economics of shale plays and other conventional reservoirs. The process of injecting a large volume of water into geothermal reservoirs increases the pore pressure and the potential of fault failure (Hubert and Rubey 1959; Cappa and Rutqvist 2011; Ellsworth 2013; Levandowski et al. 2018; Scholz 2019). From previous studies (e.g., Altmann et al. 2010; Cho et al. 2013; Taheri-Shakib et al. 2015; Cao et al. 2019), numerical simulation has become a standard method to study the behaviour of fault during injection, thus, stress and pressure build-up can be related to the fluid flow response, which could afford a better correlation with the production rate. Additionally, reports of Cho et al. 2013 described the pressure-sensitivity nature of fractured media, and how stress change influences fault permeability enhancement. However, since the tendency and magnitude of fault compaction/dilation is stress-motivated (Cappa et al. 2018), understanding the rate of change in stress distribution as the orientation of fault/joint varies can enhance the understanding of the relationship with corresponding permeability evolution and production rate.

Generally, rocks contain different geomechanical properties which change as the pore pressure changes (Eyinla and Oladunjoye 2019; Eyinla et al., 2021b). However, discontinuities also play an inevitable role in the overall mechanical and elastoplastic behaviour. The most significant types of discontinuities in rocks include faults, fractures, weak planes/joints, shear zones, planes of foliation, bedding planes, and planes of cleavage (Eshiet and Sheng, 2017). Their properties are complex, and several investigations have been carried out to assess some of their behavioural characteristics in the matrix (Brown, 1987; Fairhurst, 2013; Eshiet and Sheng, 2017; Ghosh et al., 2018). The work of Jacquey et al. (2015) explored various stimulation strategies to examine the impact of stimulation direction relative to the orientation of a pre-existing fracture network, with emphasis on the magnitude and lifespan of thermal recovery rates. In this situation, the variation in stress distribution was considered as a function of the injector position and the pressure build-up as the injection rate increases. To improve the production of geothermal energy, a sufficient amount of fracture pathway must be created, and this is only possible when fluid pressure is capable of inducing fault slip and shear deformation.

The behaviour of flow-reducing properties of rocks and overall controlling mechanism is well known through several methods including analytical, numerical (coupled flow models) or combined effects of reservoir properties including stress, pressure and fluid flow (Samaniego and Villalobos, 2003; Lei et al., 2007). Nevertheless, understanding the evolution of stress-dependent permeability in geothermal reservoir is of great interest because of the nature of the tight matrix and the fractures, which are more susceptible to stress changes (Zhang et al. 2018). Thus, the study of the variation in local stress adjacent to the wellbore and the effective stress acting normal to fracture in order to identify the initiation and propagation direction of the induced fracture would give insight into the permeability evolution, which influences production forecasting (Taheri-Shakib et al. 2015). When assessing the impact of fracture-controlled permeability reduction during production, the pressure-dependent permeability of natural fracture is often correlated with the production performance of the reservoir (Cho et al. 2013). Therefore, since the pressure distribution in the fault zone has been related to the fault properties and the hydraulic diffusivity (Rudnicki and Rice 2006; Schoenball et al. 2010; Manga et al. 2012), the energy production is partly dependent on the response of fault to the injection processes. The likelihood of hydraulic fracture intersecting natural fracture is a function of orientation, thus, the connection between the newly created fractures and pre-existing natural fractures enable adequate conclusion on why some reservoirs exhibit more complex behaviour.

Undoubtedly, simulating the THM interaction during cold fluid injection in enhanced geothermal reservoirs is crucial in evaluating the fault reactivation potential and induced seismicity (Cappa and Rutqvist, 2011). However, earlier studies by Eyinla and Oladunjoye (2021) clearly described that the frictional equilibrium of pre-existing fault is altered in a diversified range as stress redistribution in the vicinity of the fault changes, and it concluded that: (1) the effective stress in the fault zone must respond to loading before any fault failure can occur, (2) there is a direct connection between permeability changes and effective stress changes in the fault zone, (3) fluid pressure diffusion is lower at the upper part of the matrix whereas downward migration is higher, and (4) lower fault angles generally favour early onset of fault slips but the absolute effect of fault configurations is further modulated by the directions of associated joints. From these observations, this present study aims at investigating the influence of joint orientations on the production response in enhanced geothermal systems using the THM model in FLAC3D.

## Theory and methodology

The flow capacity of a reservoir is connected to its performance, and the fractures are the principal source of flow capacity (Cho et al. 2013). Thus, the existence of fractures in a reservoir are studied and characterized based on their distribution, aperture, length, orientation and spacing and weak planes connection to the fault plane. These characteristics determine the conductivity of the fractures, the distribution of pressure during injection, and the function of the effective

stress change. However, the mechanical response of a porous fractured reservoir to injection under temperature, stress and strain promotes changes in void volumes which results in permeability change (Rutqvist et al. 2002). Notably, production optimization during recovery processes would be achieved when the properties, which influence changes in pressure build-up and stress changes, are considered. One of the factors to consider in this situation is the fault/joint orientation, as the stress-dependent permeability and pressure-dependent permeability of the fault is related to the joint's orientation with respect to the fault plane and the direction of maximum principal stress. Additionally, pore pressure diffusion is highly sensitive to fracture networks and fault spatial arrangement (Prabhakaran et al. 2017).

From reports, the orientation angle of natural fracture to the normal stress is a determinant of the resulting hydraulic fracture pattern during hydraulic fracturing and dictates the permeability evolution during the cold injection. Consequently, simulating with certain fracture orientations may result in complicated hydraulic fractures (Fairhurst 2013) or low magnitude of fault slip yielding no significant permeability enhancement. Injection temperature and geometry of the fault (dip angle) hugely play an essential role in determining the permeability evolution and fault reactivation potential considering all dynamic feedbacks, where high-dip angle fractures/fault have been reported to show earlier slip than low dip angle fracture (Jacquey et al. 2015).

A distinct peculiarity of numerical approach is the ability of the designed model to produce the permeability evolution of fault in terms of frictional strength and resistance, geared by the fault's initial stability and the elastic properties. In order to estimate slip tendency along with a pre-existing fault plane, it is essential that the fault geometry is known, in terms of dip angle and dip azimuth, because the shear and effective stresses acting on a particular fault plane vary with dips (Kinoshita et al. 2019). For instance, if the angle between the fault plane and the maximum principal stress direction is large, it is expected that there would be higher shear and effective stress, consequently, a slip is more likely to occur. The instability of fault is controlled by the orientations of principal stress relative to the natural fault planes (Streit and Hillis 2004). It is thus assumed that failure may occur on the most critically oriented plane. However, the state of maximum and minimum compressive principal effective stresses is such that the fault is said to be initially stable but near a state of failure (Rutqvist and Oldenburg 2007). In this study, the Coulomb stress ratio ($\eta$) is adopted. It defines the ratio of shear stress magnitude ($\tau$) to effective normal stress magnitude ($\sigma_n'$) acting on a fault plane (Biot 1941; Byerlee 1978) as:

$$\eta = \tau / \sigma_n' \tag{1}$$

When a fault plane is subjected to a threshold level of stress during injection, a slip would occur depending on the frictional resistance of the fault and the ratio of shear to (effective) normal stress acting on that surface. While the static friction coefficient ($\mu_s$) has been defined (Cappa and Rutqvist 2011) using the friction angle ($\phi$) as $\mu_s = \tan \phi$, a slip can occur on the surface when the Coulomb stress ratio is greater than or equal to the frictional resistance to sliding (Hanks and Kanamori 1979).

Notably, one of the key roles of joints during injection is that it influences the frictional resistance of fractures and serves as a drive to improving permeability enhancement, and then impacts the production rate of the reservoir. However, a major influence of the shear strength is the cohesive strength and the frictional angle which is not only being affected by the dilation properties but also controlled by the roughness of the joint (Eshiet and Sheng 2017).

In this study, an internal fault friction angle of 28° is used, therefore, the corresponding coefficient of friction ($\mu_s$) would be 0.53 (Eq. 2), which means, for a slip to occur the critical peak friction value must be greater than or equal to 0.53 (i.e., $\eta = \tau/\sigma_n \geq \mu_s$). However, the commonly used relationship describing fault slip in the failure analysis of a fault with a specified orientation is given (Cappa and Rutqvist, 2011) as:

$$\tau = c + \mu_s \sigma_n' \tag{2}$$

And the effective stress is expressed as:

$$\sigma_n' = \sigma_n - P \tag{3}$$

where c is the cohesion, $\sigma_n$ is the total normal stress, and $P$ is the fluid pressure.

## Model description

Fracture systems in rock masses are usually complex which increases the rate of uncertainty in their quantification and analysis (Lak et al. 2017). To reduce the uncertainties, this study considers numerical simulation of fracture system for production prediction under varying patterns of discontinuities. Thus, the simulations for this study were conducted using the coupled thermo-hydro-mechanical simulator TOUGHREACT-FLAC3D, which links the TOUGHREACT multiphase flow with the FLAC3D geomechanical simulator (Itasca 2009). The coupled thermal-hydrologic-mechanical simulator considers analysis of mass and energy transport in fractured media (Pruess et al. 1999; Taron et al. 2009; Taron et al. 2009). The elastoplastic behaviour of the fault in FLAC3D which occurs as a ubiquitous fractured media impressively represent an anisotropic mechanical behaviour. A coupled hydromechanical fault model can be developed

within the framework of TOUGH–FLAC by utilizing existing capabilities within TOUGH2 and FLAC3D codes, and by developing specially designed coupling modules for faults. The fault is modelled as a ubiquitous fractured media, which accounts for the presence of an orientation of weak planes in a Mohr–Coulomb model (Cappa and Rutqvist 2011). However, this ubiquitous fault-joint model can assume distinct orientations, and their influence on the injection process in terms of permeability enhancement and magnitude of injection-induced seismicity have been fully discussed in previous reports by Eyinla et al. (2021a), and Eyinla and Oladunjoye (2021).

This study presents a simple homogenous reservoir model geometry with spatial dimension of 600 m × 15 m × 600 m ($x$, $y$, $z$), with a normal fault of length 424 m and width 2 m dipping NE at an angle 45°. Table 1 presents the assumed material properties used to populate the matrix and fault

zones during simulation. These are derived from previously published data by Eyinla (2021). Figure 1 serves as a schematic representation of the 45° fault angle, showing the assumed associated joints and their directions of dip. Fault is oriented at an angle 45° while the corresponding planes of weakness (associated joints) are chosen to be 135°, 50°, and 30°. The injection well is located at the base of the fault and the withdrawal wells at the top as shown in the model description. The initial temperature of the reservoir is assumed uniform at 180 °C. This temperature setting attempts to mimic the average temperature condition reported by Ledingham et al. (2019) for the United Downs Geothermal field.

Under normal fault kinematics, the model indicates that the vertical stress is greater than the horizontal stress; the maximum principal stress is set at 45.5 MPa ($z$-direction) while the minimum is 27.3 MPa ($x$-direction). The model

**Table 1** Material properties adopted for the numerical simulation

| Parameter (unit) | Rock matrix | Fault damage zone | Fault core |
|---|---|---|---|
| Bulk modulus (GPa) | 15 | 1.5 | 1.5 |
| Poisson's ratio | 0.22 | 0.22 | 0.22 |
| Porosity | 0.01 | 0.30 | 0.30 |
| Initial permeability (m$^2$) | $1 \times 10^{-16}$ | $1 \times 10^{-14}$ | $1 \times 10^{-15}$ |
| Rock density (kg/m$^3$) | 2700 | 2700 | 2700 |
| Heat capacity of fluid (J/kg K) | $4.26 \times 10^5$ | $4.26 \times 10^5$ | $4.26 \times 10^5$ |
| Cohesion (MPa) | 3 | 0 | 0 |
| Dilation angle (°) | 0 | 5 | 5 |
| Non-linear stiffness | – | 0.218 | 0.218 |
| Maximum aperture (m) | – | $1.52 \times 10^{-4}$ | $1.47 \times 10^{-4}$ |
| Residual aperture (m) | – | $3.03 \times 10^{-5}$ | $2.95 \times 10^{-5}$ |
| Joint cohesion MPa | – | 0 | 0 |
| Matrix friction angle (°) | 45 | 45 | 45 |
| Joint friction angle (°) | – | 28 | 28 |

**Fig. 1** A schematic representation of the model set up showing 45° fault angle and orientation of associated joints with the injector and withdrawal wells positions
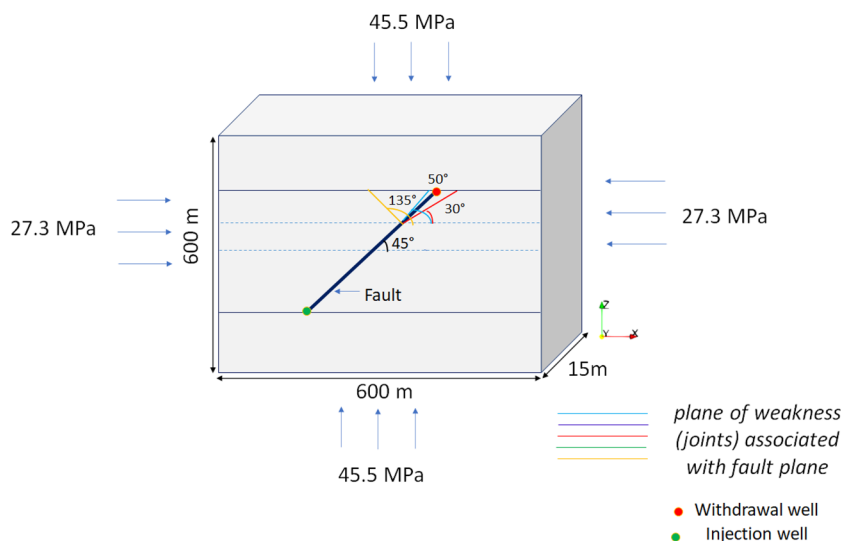
boundaries are set at no-flow boundaries, and the $y$-direction is set at roller condition with no normal displacement as constant stresses are applied. The initial pressure of the rock is set at 13.8 MPa. The fault architecture is designed with finer mesh than the other part of the reservoir. That is, the mesh size in fault and the matrix to the left and right of the fault zone contains uniform and smaller sizes than those in the other upper and lower regions of the matrix (Fig. 2a, b). This is to ensure accurate and efficient simulation of the zone of interest. In this experimental work, two different injection position scenarios are examined, and pseudo representation of the positions of the injection and withdrawal wells are shown in Fig. 2a, b. These positions are used to examine the production response as stress build-up changes. The initial permeability of the fault core is set at $10^{-15}$m$^2$, and the

damage zone is set at $10^{-14}$m$^2$. These values are greater than the initial matrix permeability, set at $10^{-16}$ m$^2$.

Notably, an interesting component of this model is the ability of the fault permeability to evolve through time. However, this permeability evolution is highly dependent on the local stress state in the reservoir, the fault's criticality to failure and the injection conditions. These would determine the fault's slip tendency, which induces the permeability enhancement during shear failure (Zoback 2007). The friction angle of the fault joint is 28° while the dilation angle is 5°, and the fracture spacing was kept constant at 0.5 m for all simulation scenarios. The fault is set to be critically stressed, dipping towards the direction of the maximum principal stress (Fig. 1). The cold water is injected at a constant injection rate of 0.1 kg/s, under constant enthalpy of



**Fig. 2** Model geometry for the reservoir with fault orientation 45° at initial condition showing two different injector positions **a** middle injection and top withdrawal, **b** bottom injection and top withdrawal
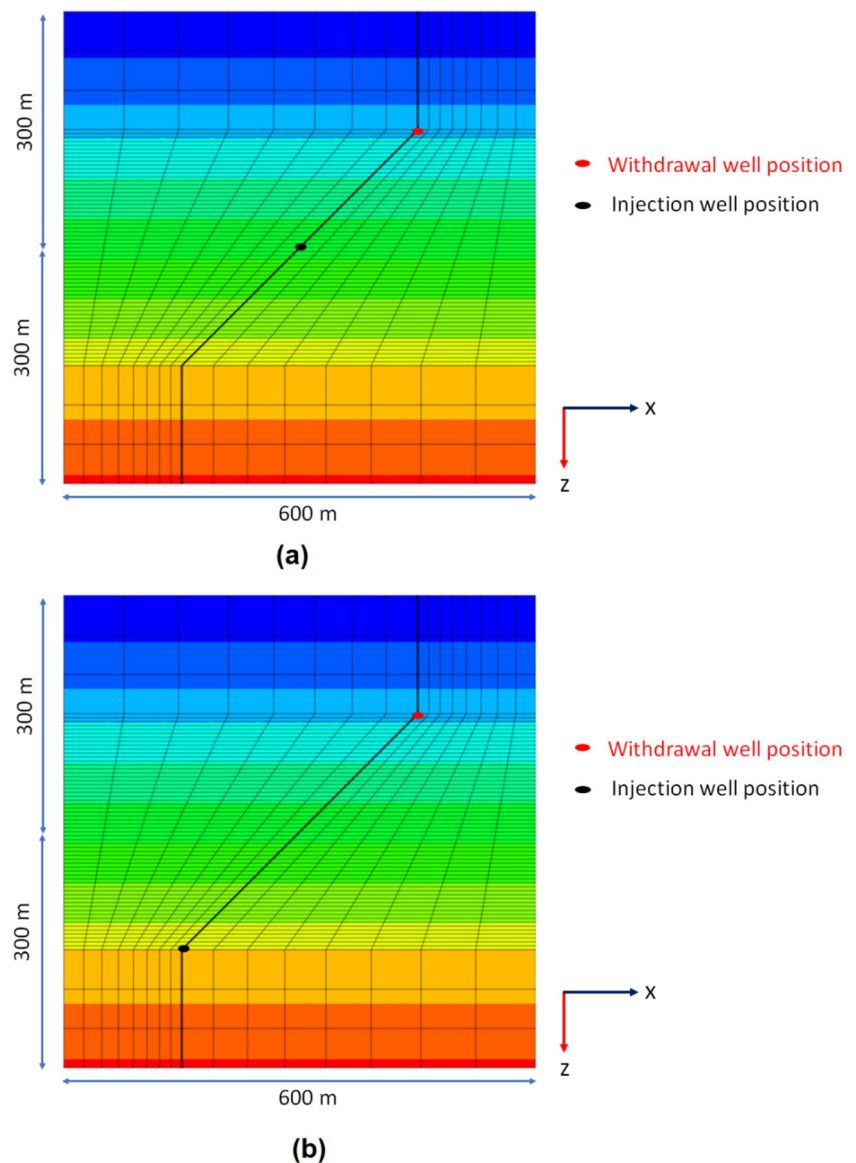
$4.26 \times 10^5$ J/kg, which is equivalent to 100 °C. This injection rate could be scaled up to a realistic value depending on the volume of the fault. However, an example for this study is the United Downs Deep Geothermal Project (UDDG) where the width of the fault damage zone varies between 400 and 600 m and aims at extracting deep geothermal energy by direct injection into the fault at a rate of about $40 - 50$ kg/s (Ledingham et al. 2019). Since the width of fault damage zone in this model is 1.2 m, it is calculated that the ratio of the UDDG fault volume to the volume of fault configuration in this study is around 400:1. Thus, the chosen injection rate in this study could be approximately scaled such that the average value of the injection rate in UDDG (45 kg/s) would give $45/400 \approx 0.1$ kg/s.

## Results and discussion

Numerical simulation of fault models under varying joint orientations have provided dissimilar permeability response during fluid injection as shown in the results obtained (Fig. 3a, b). The range of fault permeability evolution obtained here represents the response during thermo-hydro-mechanical (THM) interaction when cold fluid was injected directly into the fault without production. This response is related to the frictional resistance variation along the fault plane due to the direction of the weak planes with respect to the maximum principal stress. The result showed that when the angle between the joint and the principal stress is very large (in this case, jdip 30°), the fault tends to be relatively stable. Thus, there is no shear slip resulting from the injection process when the joint is orientated at an angle 30°, unlike the other two joint orientations, which produced shear deformation during the injection. The effect of joint at 30° orientation promotes further fault compaction, increasing frictional resistance which influences the fault plane to resist shear deformation. Therefore, as the stability becomes more enhanced in the fault plane, fault slip tendency is lowered (Jacquey et al. 2015). The tendency and magnitude of seismicity during injection has been ascribed to the injection fluid conditions and the fault initial stability with respect to the orientation and the frictional stability of the joints.
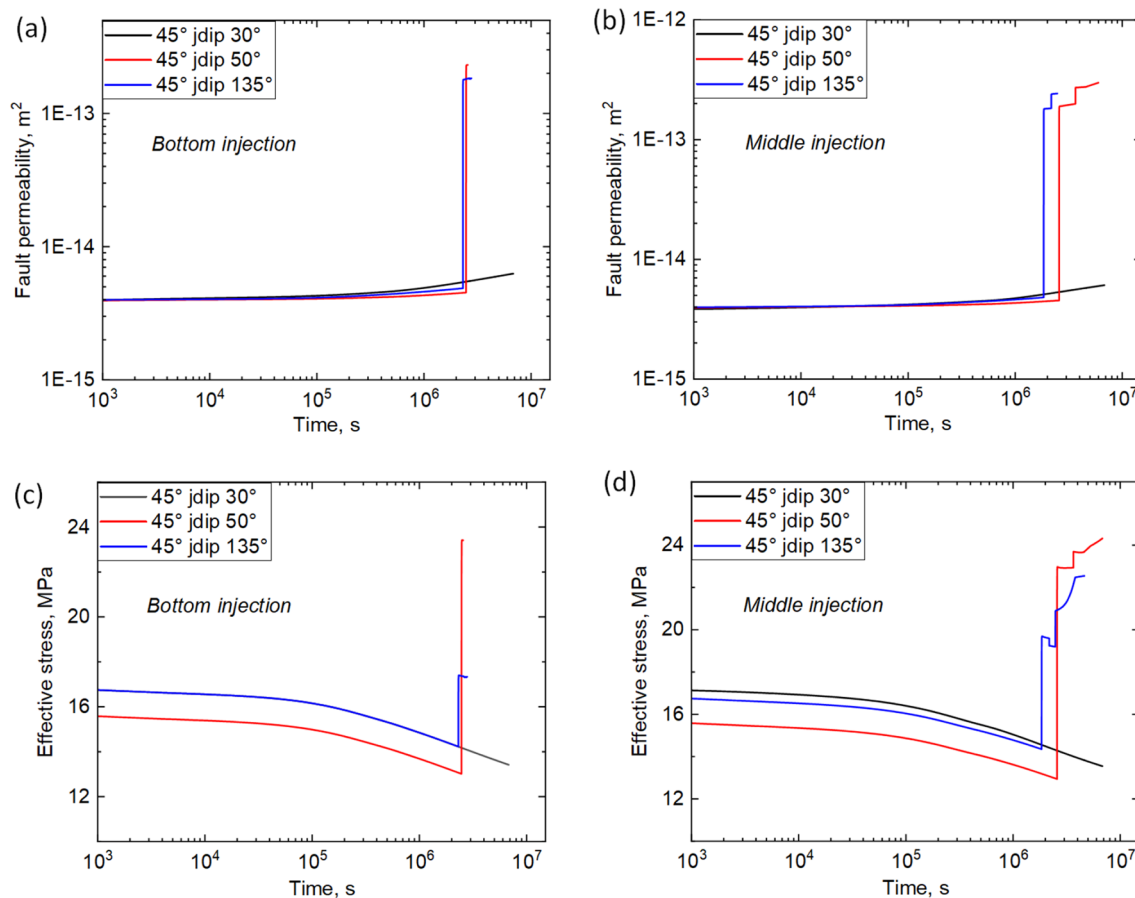


**Fig. 3** **a**, **b** Stress-induced permeability enhancement and the evolution of effective stress for the various joint orientations at bottom injection **c**, **d** Stress-induced permeability enhancement and the evolution of effective stress for the various joint orientations at the middle injection

Notably, joint dip 50° produced the highest permeability enhancement among the joint directions, invariably, the most unstable of the three fault models, as also reported by Eyinla and Oladunjoye (2021). This implies that other factors (e.g., elastic constants, injection rate, initial fault-matrix permeability) being constant, the tendency of fault rupture during injection is proportional to the direction of joints with respect to the maximum principal stress direction. This also directly relates to the permeability evolution. Evidently, the most significant fault permeability enhancement is only observed when there is a shear slip. Thus, slip tendency and slip magnitude of faults becomes a major concern in ensuring successful injection and production.

Permeability enhancement is strongly affected by the joint orientation in the model, as it determines the stress state during injection (Fig. 3c, d). The observation here is that the response of each fault/joint model to stress change varies, and this influenced the possibility of having different levels of fault criticality to failure. In joint angle 50°, there is an increasing rate of stress drop during unloading than what is observed in angle 135°. This produced a strong effect on the permeability evolution, which is highly stress-induced. However, a comparison of the effects of joint orientation during production has also revealed that there is a significant difference in production rate at changing joint directions (Figs. 4,5,6). Apparently, the evolution of pore pressure in each joint model produced a curve which is an exact replica of the production rate curve (Figs. 4,5,6). This could imply that energy production from geothermal reservoir is highly dependent on the pressure distribution during injection, such that as pressure rises or falls, the production rate follows the same trend and vice versa.

Notably, the change in fault permeability following the shear failure on the fault plane vary in timing and magnitude as the fault geometry and the injection position change. An
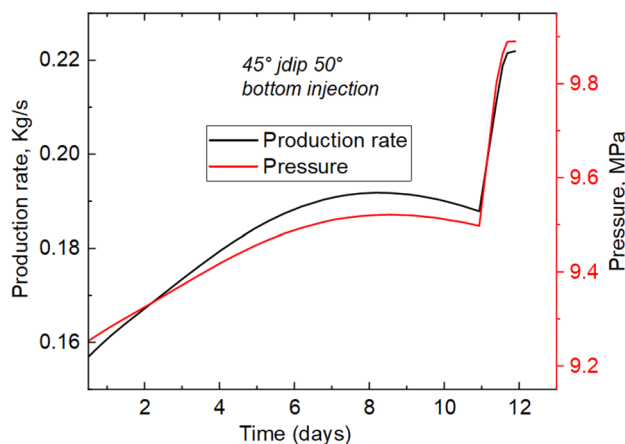
**Fig. 5** Production response and pressure evolution with joint orientation 50°

observation which has been established in this study and previous reports (e.g., Eyinla et al. 2020, 2021a; Eyinla and Oladunjoye 2021). However, because the injection-induced permeability provides a pathway through which migration of fluid can occur, the production rate is expected to be directly related to the injection-induced permeability. From the results obtained, it is deduced that the possibility and/or magnitude of shear-induced permeability evolution is directly related to the production rate evolution, such that the fault model with little or no tendency of fault rupture under injection would produce lower energy rate. Meanwhile, under the same injection conditions, the fault/joint configuration with higher magnitude of slip displacement and permeability enhancement has the tendency of producing higher flow rate. In jdip 50° which has the most enhanced fault opening and shear-induced permeability, the corresponding production rate is highest (Fig. 5) when compared to the
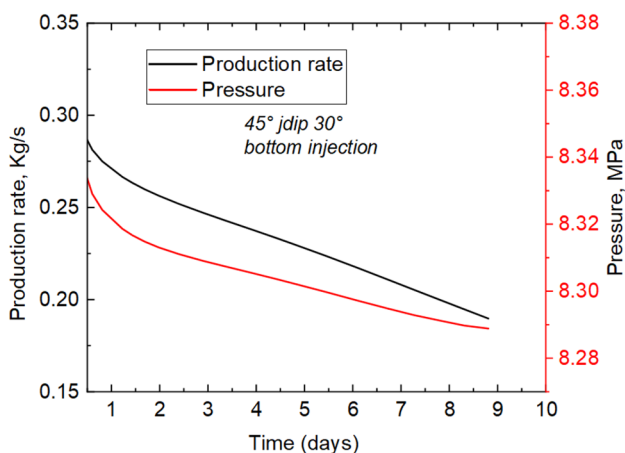
**Fig. 4** Production response and pressure evolution with joint orientation 30°
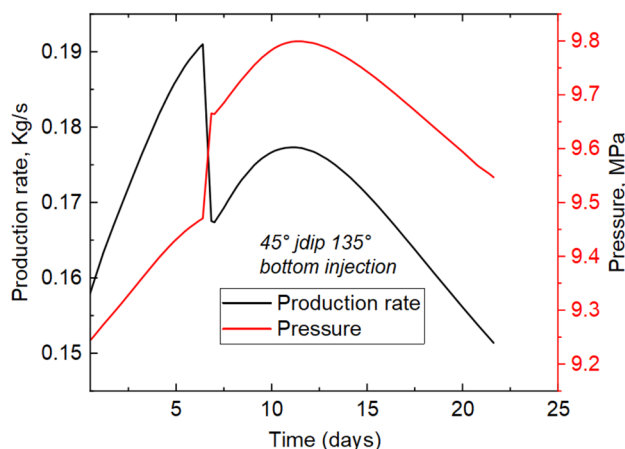
**Fig. 6** Production response and pressure evolution with joint orientation 135°

other two joint directions (Figs. 4,6). This literally means that in agreement with the report by Fan et al. (2016), the increased volume of migration pathways would impact on the production rate. The production curve in jdip 30° indicates a decreasing rate till simulation terminates after 9 days of injection (Fig. 4). The curve of jdip 50° on the other hand yielded a continuous rise in production rate from the onset of injection till after 11 days when there was a sudden rise to 0.23 kg/s before simulation terminates. Nevertheless, jdip 135° indicates an increasing and decreasing progression of production rate which eventually falls to about 0.15 kg/s before simulation ends. Most often, fractured reservoir with a higher potential of slip has potential for an earlier onset of seismic activity (Fan et al. 2016). However, in all the cases examined, the potential for seismicity varies, but the highest is recorded in joint orientation 50° with moment magnitude, Mw of about 1.5, indicating low seismicity.

## Influence of stress and pore pressure change on production rate

As discussed in the preceding section, pore pressure in the fault zone gives a corresponding trend as the production rate and vice versa. Thus, the evolution of the pressure build-up controls the seepage capability of the fractured reservoir. Figures 7, 8 and 9 show the contour of pore pressure distribution at the end of simulation for the three joint orientations. These show that the base of the reservoir is more pressured while pressure is lower at the top. However, the point where the withdrawal well is located had experienced pressure drawdown, because, at this location, pressure is lowest as indicated on the contour plot.

This result is compared with the work of Zhang et al. (2018) which had reported that stress-dependent permeability determines the production rates to a certain level, and the rate is highly dependent on the level of wellbore flowing pressure. Thus, in stress-sensitive reservoir, production is tied to additional pressure drawdown, which will result in pressure-dependent production. Although the values of production rates are impacted by improved stress-sensitive permeability, the overall character of the production rate curve is one, which is related to the pressure curve. Therefore, changes in effective stress generate undrained fluid pressure increments leading to a consequent change in production response (Taron et al. 2009).

It is observed that pore pressure elevation is not the only cause of shear failure, as the change in effective stress has been described as an important factor, which influences fault slip. Additionally, thermal stress has been verified as the cause of the enhanced slip and permeability enhancement during cold injection (Eyinla and Oladunjoye 2021). Although the thermal influence induces late-stage seismic slip as a result of thermal drawdown, it has been reported to be a major source of large magnitude seismicity (Ghassemi



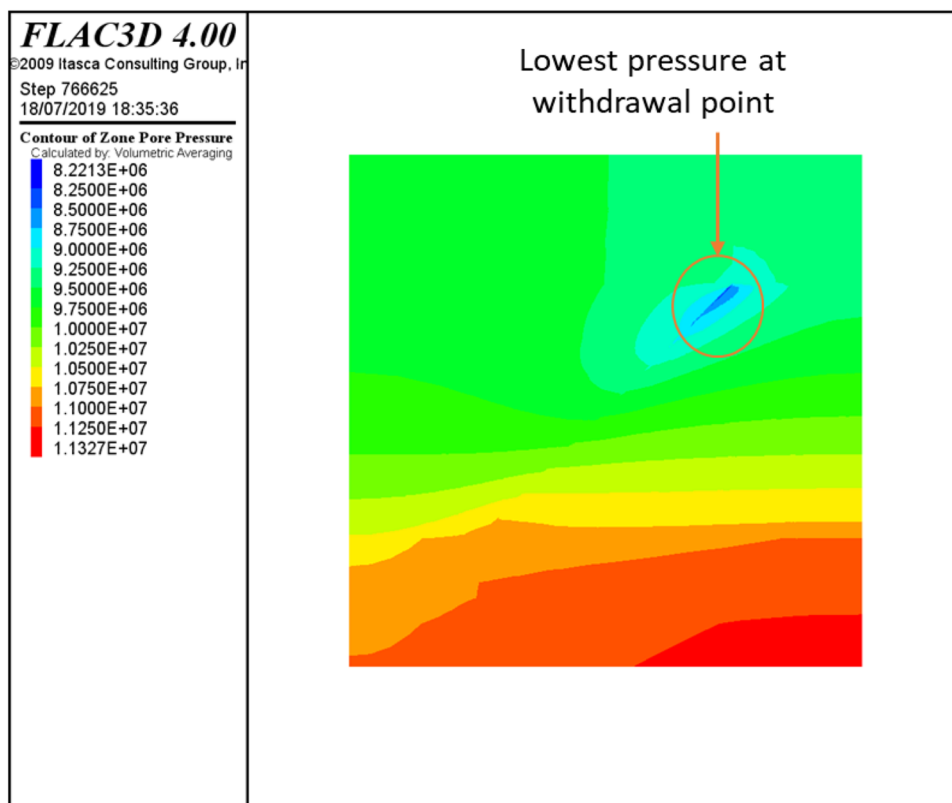**Fig. 7** Contour of Pore pressure distribution for joint orientation 30° after simulation

**Fig. 8** Contour of Pore pressure distribution for joint orientation 50° after simulation
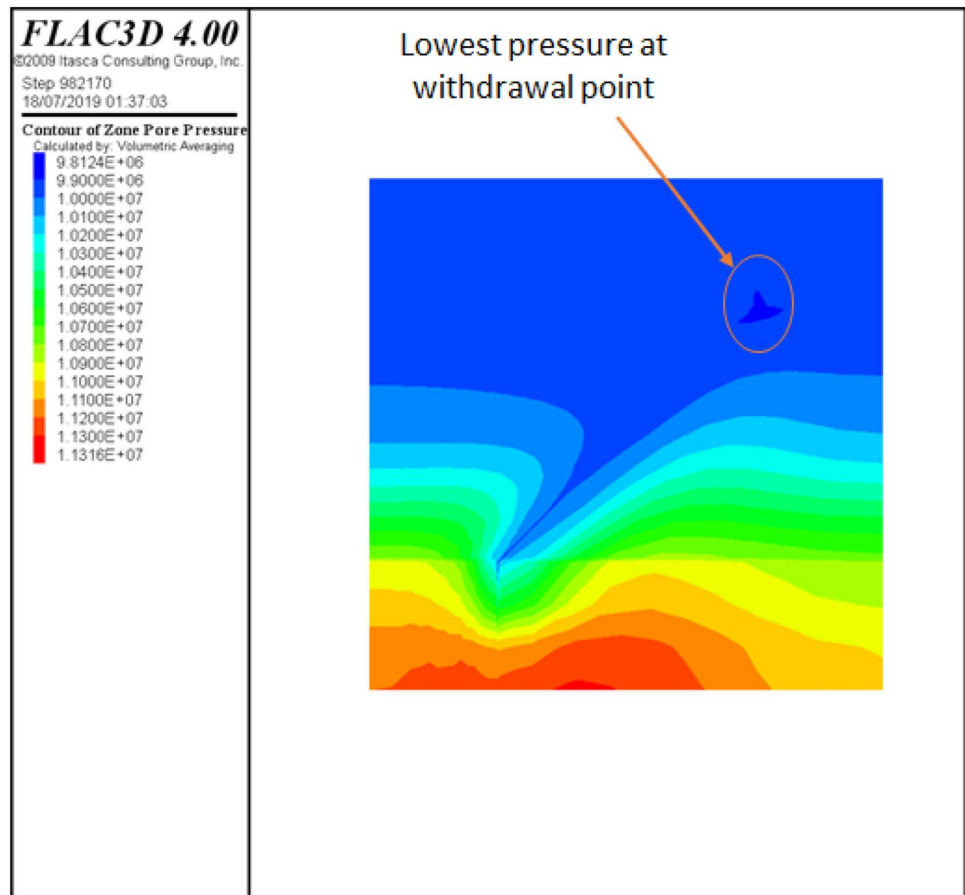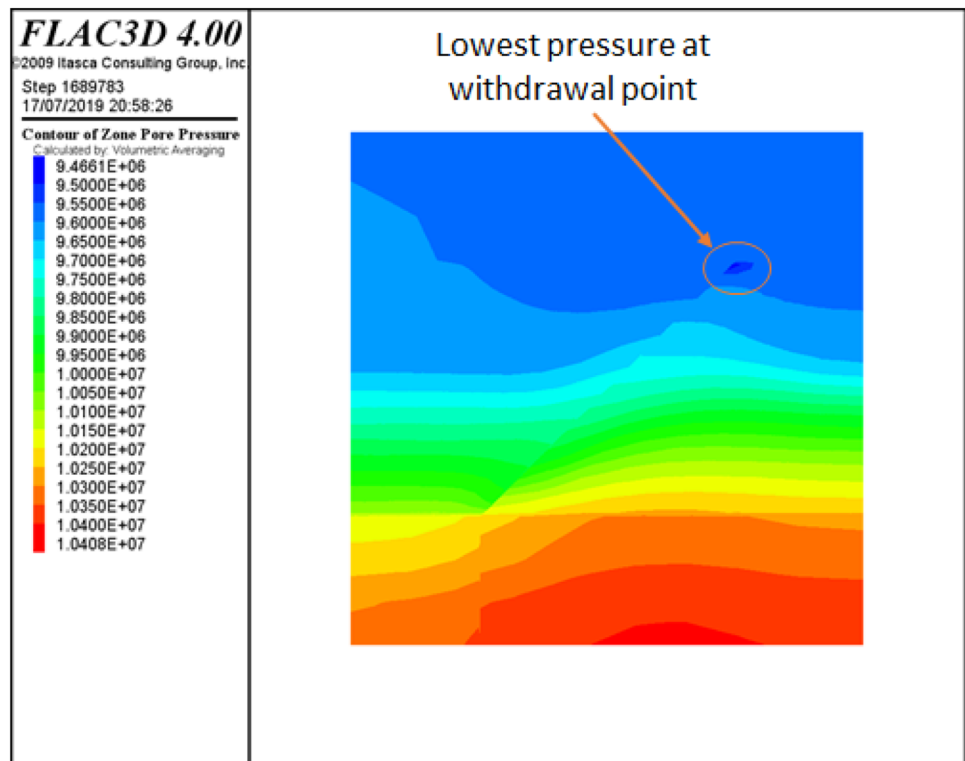


**Fig. 9** Contour of Pore pressure distribution for joint orientation 135° after simulation

and Tarasovs, 2007; De Simone et al. 2013; Jeanne et al. 2015). Structurally, fault opens during fluid injection, and the implication of this is that permeability variation and production rate is closely proportional to the evolution of fluid pressure (Rutqvist and Stephansson 2003; Cappa et al. 2007; Guglielmi et al. 2015).

Figure 10a–f show the production plots for the three fault/joint configurations at the two different injection positions

in Fig. 2a and b. The first case involves the injection of cold fluid at the base of the fault (bottom injection), and the second scenario involves injection at the centre of the fault (middle injection). The withdrawal well is fixed at the same position which is at the top end of the fault. The results obtained demonstrate the effects of the state of stress at the locations of the injection and withdrawal wells on the production rate. For the two injection position cases considered,
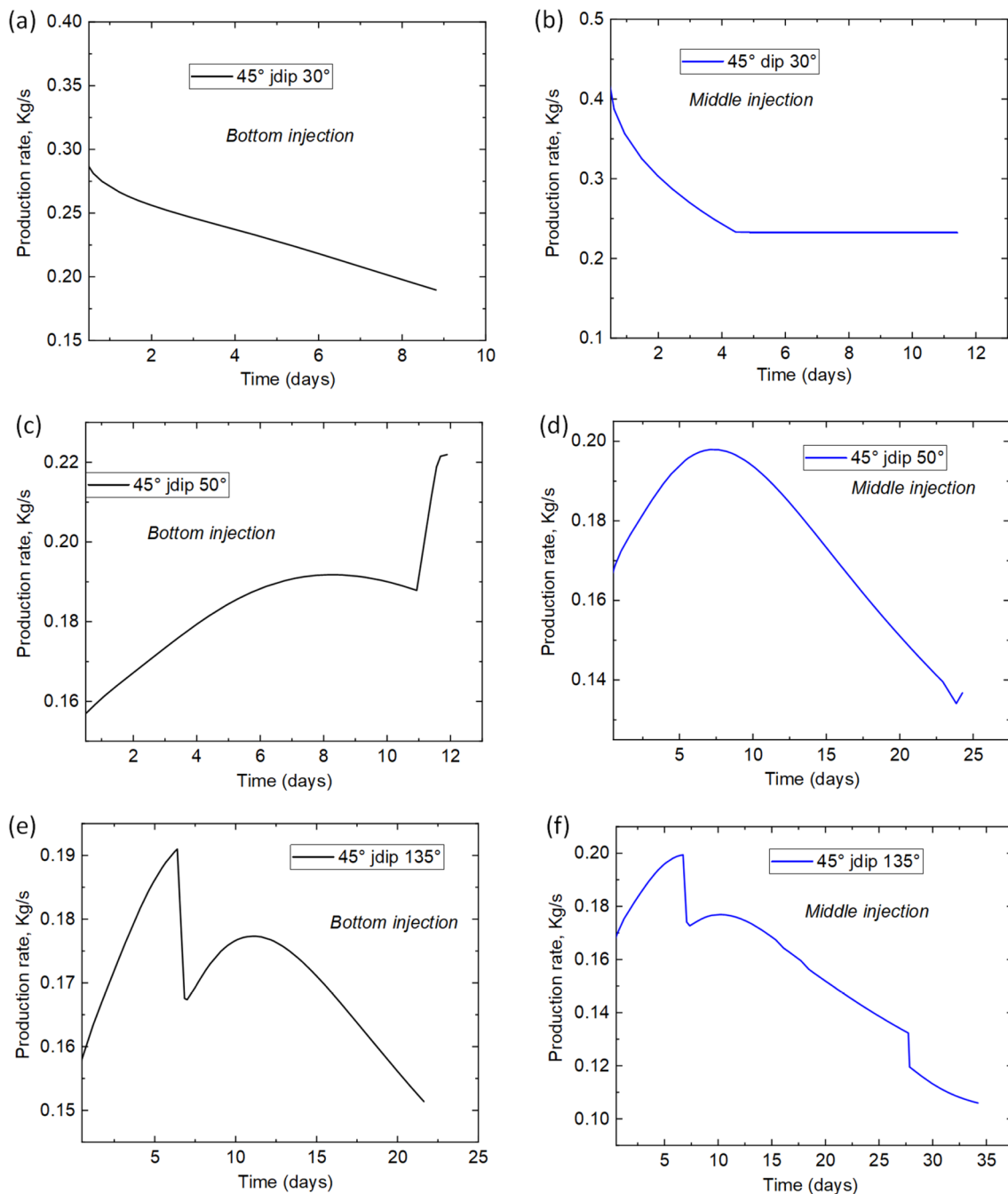


**Fig. 10** Comparison of production evolution under different injection position and changing joint orientations **a**, **b** jdip 30° bottom and middle injection **c**, **d** jdip 50° bottom and middle injection **e**, **f** jdip 135° bottom and middle injection

the production evolution is primarily influenced by the prevailing stress change in the reservoir. Thus, the state of stress at the locations of the injection and production wells produced a huge influence on the production flow rate. This is also related to the evolution of fault permeability as shear failure occurs, implying that the state of stress at the injection well influences the pressure distribution at the withdrawal well. There is a significant variation in the production rate for the two injector positions as observed with the three fault/joint configurations. This indicates that the position of injection has a first-order control on the growth of production cycle, which could be linked to the diffusivity potential of fluid pressure. Seemingly, this is expected to influence the evolution of electrical power generation in each model.

Injecting at the centre of the fault afforded a longer production cycle in the three joint models, whereas injection at the base of the fault yielded a higher rate, especially in jdip 50°. Generally, middle injection shows decreasing rate of production with time but with longer production time, and this is more evident in jdip 50°. Thus, it is proposed that with the injector positioned at the base of the fault, there is a more energetic event and complex interplay which occurs during the phase of hydraulic connection between the injector well and the withdrawal due to the relative distance between the two points. Relatively, the pore pressure evolution in these two scenarios was elevated differently throughout the injection period. Also, the state of stress at the location of the injection well plays a significant role in determining the time of slip on the fault plane and hence the permeability evolution. The evolution of production or flow rate is also influenced by the state of stress at the locations of the injection and production wells would in turn influence the evolution of electrical power generation.

## Conclusions

This study has described the behaviour of faulted reservoir under stress and pressure distribution in terms of permeability evolution, and the influence of these on the performance geothermal reservoir during production. Thermo-hydro-mechanical simulation involving different joint patterns has revealed an incredible variation in the corresponding permeability evolution and production response through coupled discrete fracture modelling. The injection response of the varying plane of weakness (joints) in this study indicates how changes in the position of weak planes with respect to the direction of the maximum principal stress impacts the injection and withdrawal processes. The following conclusions were drawn from this study:

1. Fault/joint orientation is observed to be an important factor in influencing the stimulation result, both in permeability evolution and production optimization.

2. The absolute effect of fault configurations is modulated by the directions of associated joints on their planes. For example, because jdip 30° confer special stability on the fault plane during injection by resisting fault slip, the permeability enhancement is retarded, thus the production rate is low.

3. The production rate in jdip 30° is followed by jdip 135°, a joint model which although produced fault slip but yielded lower magnitude when compared with jdip 50°. Thus, the highest magnitude of permeability enhancement is observed in joint orientation 50°, and this is directly related to the production rate.

4. Additionally, the pressure evolution curve produced an exact replica of the production rate curve, which indicates that the two are directly related. A drop in the production rate implies that the pore pressure would be lowered while an increasing trend of production rate means pressure elevation.

5. Also, thermal drawdown is enhanced when the effect of thermal stress is high, as the various output is driven by the magnitude of pressure diffusion and thermal mechanisms causing sufficient cooling of the reservoir.

6. The resultant pressure and stress evolution are affected by the position of the injection well, as bottom injection appears to yield a more significant production evolution than middle injection.

7. Also, the potential of fault reactivation and fracture opening is influenced by the mechanism of stress change. Overall, the magnitude of shear-induced permeability influences the evolution of production flow rate and this is dependent on the stress state at the injection and withdrawal point.

Thus, for well development and well placement, the results from this study would afford a better guidance during energy production from geothermal reservoir where the complex state of the fractures could cause variations in fault/joint orientations. This knowledge would also help in improving the reservoir performance to ensure production optimization.

## Declarations

**Conflict of interest** The author declares that there is no conflict of interest.

**Open Access** This article is licensed under a Creative Commons Attribution 4.0 International License, which permits use, sharing, adaptation, distribution and reproduction in any medium or format, as long as you give appropriate credit to the original author(s) and the source, provide a link to the Creative Commons licence, and indicate if changes were made. The images or other third party material in this article are included in the article's Creative Commons licence, unless indicated otherwise in a credit line to the material. If material is not included in the article's Creative Commons licence and your intended use is not permitted by statutory regulation or exceeds the permitted use, you will need to obtain permission directly from the copyright holder. To view a copy of this licence, visit http://creativecommons.org/licenses/by/4.0/.

## References

Altmann JB, Müller TM, Müller BIR, Tingay MRP (2010) Heidbach O (2010) Poroelastic contribution to the reservoir stress path. Int J Rock Mech Min Sci 47(7):1104–1113. https://doi.org/10.1016/j.ijrmms.2010.08.001

Biot MA (1941) General theory of three-dimensional consolidation. J Appl Phys 12(2):155–164. https://doi.org/10.1063/1.1712886

Brown SR (1987) Fluid flow through rock joints: the effect of surface roughness. J Geophys Res 92(B2):1337–1347. https://doi.org/10.1029/JB092iB02p01337

Byerlee J (1978) Friction of Rocks. Pure Appl Geophys PAGEOPH 116(4–5):615–626. https://doi.org/10.1007/bf00876528

Cao N, Lei G, Dong P, Li H, Wu Z, Li Y (2019) Stress-dependent permeability of fractures in tight reservoirs. Energies 12(1):117. https://doi.org/10.3390/en12010117

Cappa F, Rutqvist J (2011) Modeling of coupled deformation and permeability evolution during fault reactivation induced by deep underground injection of CO2. Int J Greenhouse Gas Control 5(2):336–346. https://doi.org/10.1016/j.ijggc.2010.08.005

Cappa F, Guglielmi Y, Virieux J (2007) Stress and fluid transfer in a fault zone due to overpressures in the seismogenic crust. Geophys Res Lett 34(5). https://doi.org/10.1029/2006GL028980

Cappa F, Guglielmi Y, Nussbaum C, Birkholzer J (2018) On the relationship between fault permeability increases, induced stress perturbation, and the growth of aseismic slip during fluid injection. Geophys Res Lett 45(20):11012–11020. https://doi.org/10.1029/2018GL080233

Cho Y, Apaydin OG, Ozkan E (2013) Pressure-dependent natural-fracture permeability in shale and its effect on shale-gas well production. Published in 2013. Presented at SPE Annual Technical Conference and Exhibition, San Antonio, Texas, USA, pp 8–10

De Simone S, Vilarrasa V, Carrera J, Alcolea A, Meier P (2013) Thermal coupling may control mechanical stability of geothermal reservoirs during cold water injection. Phys Chem Earth 64:117–126. https://doi.org/10.1016/j.pce.2013.01.001

Ellsworth WL (2013) Injection-induced earthquakes. Science 341(6142):122592

Eshiet KII (Aug. 2017) Sheng Y (2017) The role of rock joint frictional strength in the containment of fracture propagation. Acta Geotech 12(4):897–920. https://doi.org/10.1007/s11440-016-0512-2

Eyinla DS (2021) Modelling of fault reactivation mechanisms and associated induced seismicity in rocks with different elastic materials. Petroleum Res. https://doi.org/10.1016/j.ptlrs.2021.07.001

Eyinla DS, Oladunjoye MA (2019) Empirical analysis for the characterization of geo-mechanical strength and pressure regime: Implications on hydraulic fracturing stimulation. Petroleum 5(3). https://doi.org/10.1016/j.petlm.2018.05.002

Eyinla DS, Oladunjoye MA (2021) Controls of thermal stress on fault slip modes: implications for injection induced seismicity and permeability enhancement. Petroleum Res. https://doi.org/10.1016/j.ptlrs.2021.05.002

Eyinla DS, Oladunjoye MA, Gan Q, Olayinka AI (2020) Fault reactivation potential and associated permeability evolution under changing injection conditions. https://doi.org/10.1016/j.petlm.2020.09.006

Eyinla DS, Gan Q, Oladunjoye MA (2021a) Olayinka AI (2021a) Numerical investigation of the influence of discontinuity orientations on fault permeability evolution and slip displacement. Geomech Geophys Geo-Energ Geo-Resour 7:36. https://doi.org/10.1007/s40948-021-00236-7

Eyinla DS, Oladunjoye MA, Olayinka AI, Bate BB (2021b) Rock physics and geomechanical application in the interpretation of rock property trends for overpressure detection. J Pet Explor Prod Technol 11(2021):75–95. https://doi.org/10.1007/s13202-020-01039-4

Fairhurst C (2013) Fractures and fracturing: hydraulic fracturing in jointed rock. ISRM international conference for effective and sustainable hydraulic fracturing, pp. 47–79. https://doi.org/10.5772/56366

Fan Z, Eichhubl P, Gale JFW (2016) Geomechanical analysis of fluid injection and seismic fault slip for the Mw4.8 Timpson, Texas, earthquake sequence. J Geophys Res Solid Earth 121(4):2798–2812. https://doi.org/10.1002/2016JB012821

Ghassemi A, Tarasovs S (2007) Cheng AHD (2007) A 3-D study of the effects of thermomechanical loads on fracture slip in enhanced geothermal reservoirs. Int J Rock Mech Min Sci 44(8):1132–1148. https://doi.org/10.1016/j.ijrmms.2007.07.016

Ghosh S, Milad B, Prasun S, Gosh S (2018) Origin and characterization of joints in sedimentary rocks: a review. Petroleum Petrochem Eng J 2(5):1–12

Guglielmi Y, Cappa F, Avouac JP, Henry P, Elsworth D (2015) Seismicity triggered by fluid injection-induced aseismic slip. Science 348(6240):1224–1226. https://doi.org/10.1126/science.aab0476

Hanks TC (1979) Kanamori H (1979) A moment magnitude scale. J Geophys Res B Solid Earth 84(B5):2348–2350. https://doi.org/10.1029/JB084iB05p02348

Hubbert MK, Rubey W (1959) Role of fluid pressure in mechanics of overthrust faulting. Geol Soc Am Bull 70(1959):115–205. https://doi.org/10.1130/0016-7606(1959)70[115:ROFPIM]2.0.CO;2

Itasca F (2009) Fast Lagrangian Analysis of Continua (FLAC) Version 4.00 (A two-dimensional explicit finite difference program for engineering mechanics computation.). Itasca Consulting Group, Minnesota

Jacquey AB, Cacace M, Blöcher G, Scheck-Wenderoth M (2015) Numerical investigation of thermoelastic effects on fault slip tendency during injection and production of geothermal fluids. Energy Procedia 76:311–320. https://doi.org/10.1016/j.egypro.2015.07.868

Jeanne P, Rutqvist J, Dobson PF, Garcia J, Walters M, Hartline C, Borgia A (2015) Geomechanical simulation of the stress tensor rotation caused by injection of cold water in a deep geothermal reservoir. J Geophys Res Solid Earth 120(12):8422–8438. https://doi.org/10.1002/2015JB012414

Kinoshita M, Shiraishi K, Demetriou E, Hashimoto Y, Lin W (2019) Geometrical dependence on the stress and slip tendency acting on the subduction megathrust of the Nankai seismogenic zone off Kumano. Prog Earth Planet Sci 6(1). https://doi.org/10.1186/s40645-018-0253-y

Lak M, Baghbanan A, Hashemolhoseini H (2017) Effect of seismic waves on the hydro-mechanical properties of fractured rock masses. Earthq Eng Eng Vib 16(3):525–536. https://doi.org/10.1007/s11803-017-0406-9

Lavrov A (2017) (2017) Fracture permeability under normal stress: a fully computational approach. J Pet Explor Prod Technol 7:181–194. https://doi.org/10.1007/s13202-016-0254-6

Ledingham P, Cotton L, Law R (2019) The United Downs Deep Geothermal Project, in: 44th Work. Geotherm. Reserv. Eng. https://www.uniteddownsgeothermal.co.uk/.

Lei Q, Xiong W, Yuang J, Cui Y, Wu Y (2007) Analysis of stress sensitivity and its influence on oil production from tight reservoirs. doi: https://doi.org/10.2118/111148-MS.

Levandowski W, Weingarten M, Walsh R (2018) Geomechanical sensitivities of injection-induced earthquakes. Geophys Res Lett 45(17):8958–8965

Manga M, Beresnev I, Brodsky EE, Elkhoury JE, Elsworth D, Ingebritsen SE, Mays DC, Wang C-Y (2012) Changes in permeability caused by transient stresses: field observations, experiments, and mechanisms. Rev Geophys 50(2). https://doi.org/10.1029/2011RG000382

Men X, Li J, Han Z (2018) Fracture propagation behavior of jointed rocks in hydraulic fracturing

Prabhakaran R, de Pater H, Shaoul J (2017) Pore pressure effects on fracture net pressure and hydraulic fracture containment: Insights from an empirical and simulation approach. J Petrol Sci Eng 157:724–736. https://doi.org/10.1016/j.petrol.2017.07.009

Pruess K, Oldenburg C, Moridis G (1999) TOUGH2 user's Guide, version 2

Rudnicki JW, Rice JR (2006) Effective normal stress alteration due to pore pressure changes induced by dynamic slip propagation on a plane between dissimilar materials. J Geophys Res Solid Earth 111(10). https://doi.org/10.1029/2006JB004396

Rutqvist J (2003) Stephansson O (2003) The role of hydrochemical coupling in fractured rock engineering. Hydrogeol J 11(1):7–40. https://doi.org/10.1007/s10040-002-0241-5

Rutqvist J, Oldenburg C (2007) Analysis of cause and mechanism for injection-induced seismicity at the Geysers geothermal field, California. GRC Trans 31:441–445

Rutqvist J, Wu YS, Tsang CF, Bodvarsson G (2002) A modeling approach for analysis of coupled multiphase fluid flow, heat transfer, and deformation in fractured porous rock. Int J Rock Mech Min Sci 39:429–442

Samaniego VF, Villalobos LH (2003) Transient pressure analysis of pressure-dependent naturally fractured reservoirs. J Petrol Sci Eng 39(1–2):45–56. https://doi.org/10.1016/S0920-4105(03)00039-1

Schoenball M, Müller TM, Müller BIR, Heidbach O (2010) Fluid-induced microseismicity in pre-stressed rock masses. Geophys J Int 180(2):813–819. https://doi.org/10.1111/j.1365-246X.2009.04443.x

Scholz CH (2019) The mechanics of earthquakes and faulting, 3rd edn. Cambridge University Press, Cambridge, UK

Streit JE, Hillis RR (2004) Estimating fault stability and sustainable fluid pressures for underground storage of CO2 in porous rock. Energy 29(9–10):1445–1456. https://doi.org/10.1016/j.energy.2004.03.078

Taheri-Shakib J, Akhgarian E, Ghaderi A (2015) The effect of hydraulic fracture characteristics on production rate in thermal EOR methods. Fuel 141:226–235. https://doi.org/10.1016/j.fuel.2014.10.063

Taron J (2009) Elsworth D (2009) Thermal-hydrologic-mechanical-chemical processes in the evolution of engineered geothermal reservoirs. Int J Rock Mech Min Sci 46(5):855–864. https://doi.org/10.1016/j.ijrmms.2009.01.007

Taron J, Elsworth D, Min KB (2009) Numerical simulation of thermal-hydrologic-mechanical-chemical processes in deformable, fractured porous media. Int J Rock Mech Min Sci 46(5):842–854. https://doi.org/10.1016/j.ijrmms.2009.01.008

Vilarrasa V, Makhnenko R, Gheibi S (2016) Geomechanical analysis of the influence of CO2 injection location on fault stability. J Rock Mech Geotech Eng 8(2016):805–818

Zhang Z, He S, Gu D, Gai S, Li G (2018) Effects of stress-dependent permeability on well performance of ultra-low permeability oil reservoir in China. J Petrol Exp Prod Technol 8(2):565–575. https://doi.org/10.1007/s13202-017-0342-2

Zoback MD (2007) Reservoir geomechanics. Cambridge university press

**Publisher's Note** Springer Nature remains neutral with regard to jurisdictional claims in published maps and institutional affiliations.